

Numerical modeling for slope stability analysis: a case study of the landslide on RN12 at PK 119+000, Adegar, Béjaïa, Algeria

Badreddine Bousbia^{1,*}, Kamel Goudjil²

¹ Higher Normal School of Technological Education, of Skikda, Algeria; b.bousbia@enset-skikda.dz

² Laboratory INFRARES, Mohammed Cherif Messaadia University, Souk-Ahras, Algeria; k.goudjil@univ-soukahras.dz

* Corresponding Author

Received: 31.07.2025; Revised: 23.01.2026; Accepted: 28.01.2026; Available online: 31.03.2026

License: CC-BY 4.0; 2026 Budownictwo i Architektura – Civil and Architectural Engineering

Abstract:

One of the biggest geotechnical risks is landslides, particularly in areas with mountains and seismic activity. This study focuses on soil reinforcement to a variety of methods intended to enhance the mechanical or physical characteristics of the ground by adding inclusions that function in tension, compression, or bending, in light of the technical and financial constraints of conventional retaining wall systems. Among these methods, soil nailing has become a cutting-edge, practical, and flexible stabilization technique. Investigating landslide-induced slope failures and suggesting site-specific soil improvement strategies that increase safety and reduce displacements are the goals of this study. Because landslides occur frequently in the area, a slope along a road in the commune of ADEKAR in the Béjaïa province (Algeria), was chosen as the case study site for this investigation. Two-dimensional finite element analysis (FEA) was used to evaluate the slope's stability. This study shows that using soil nailing reinforcement techniques in conjunction with numerical modeling is a viable and effective stabilization method.

Keywords:

slope stability; soil nailing, slip, circle failure, factor of safety, GTS NX software, numerical modeling

1. Introduction

Landslides are defined as the movement of a mass of unconsolidated or rocky terrain along a shear failure surface. Their occurrence depends on the nature and arrangement of geological layers and is driven by gravity, external forces (such as hydraulic or seismic forces), or changes in boundary conditions [1-3]. Landslides typically involve slow displacements ranging from a few millimeters per year to several meters per day of a coherent soil mass along a curved or planar failure surface [4]. Mudflows, which often originate in the lower parts of landslides, represent the evolved stage of these movements and consist of rapid flows of remobilized materials. Fundamentally, the mechanics of such ground movements are well understood: they occur when the resisting strength of soil or rock becomes lower than the driving forces induced by gravity, groundwater pressure, or anthropogenic activities. Their behavior adheres to the principles of classical mechanics [5-7]. In Algeria, landslides are among the most frequently occurring geological hazards [8], especially in the province of Béjaïa. Despite receiving less media attention than earthquakes or volcanic eruptions, these phenomena cause significant damage to infrastructure and entail considerable economic costs [9]. This field of research at the intersection of soil mechanics, structural analysis, and geodynamics has experienced substantial development over the past few decades, largely in response to the rising frequency of natural disasters related to landslides [10,11].

It is now more important than ever to have effective tools for slope analysis, prediction, and stabilization. Traditional retaining methods such as reinforced concrete walls, gabions, and sheet piles have proven to be effective, yet they also present notable limitations: high costs, large spatial footprint, and implementation challenges in rugged or saturated terrains

[12,13]. Simultaneously, the more recent in situ soil reinforcement techniques have become very popular. Among these, soil nailing has become a novel, adaptable, and economical solution that works especially well for loose or unstable soils [14-16].

Widely adopted for the stabilization of weak or unstable slopes, soil nailing employs steel tendons embedded within the soil mass to reinforce its structural integrity. In contrast to active anchoring systems, these tendons are not pre-tensioned; rather, they become progressively engaged as the surrounding soil deforms. This controlled mobilization facilitates effective load transfer along the soil–nail interface, enhancing shear resistance and overall slope stability. The technique proves particularly efficient for loose, cohesionless, or otherwise geotechnical vulnerable soils, offering both immediate reinforcement and long-term resilience under operational loading conditions. The system relies on the installation of slightly inclined steel bars, typically drilled into the slope and subsequently grouted using cement slurry or injected under pressure [17]. Each nail is connected to the surface to a shotcrete facing by means of an anchorage plate and bolting system, which ensures the transfer of stresses. When the soil begins to deform, the resulting forces acting on the facing are transmitted to the nails, which operate in tension to stabilize the slope [18]. This mechanism reinforces the soil mass by mobilizing its internal strength while preserving its structural integrity. It has been demonstrated that increasing the length of the nails significantly improves the safety factor by expanding the anchorage influence zone and optimizing stress distribution within the reinforced soil. This method has proven effective in a variety of infrastructure projects, including mountain roads, deep urban excavations, embankment structures, and natural slopes [19,20].

However, the optimal design of such systems relies on a thorough understanding of soil-structure interactions, as well as precise control of local geotechnical parameters. Indeed, performing soil nailing depends highly on factors such as nail length, horizontal and vertical spacing, inclination relative to the horizontal, and the mechanical properties of the soil, including cohesion, Young's modulus, and internal friction angle [21]. A combined analysis of these parameters requires the use of advanced numerical modeling tools capable of capturing the complex mechanisms governing the behavior of reinforced slopes [22].

In this context, developments in geotechnical simulation software have constituted a significant breakthrough. Among these tools, MIDAS GTS NX stands out for its extensive two-dimensional modeling capabilities. This study provides a detailed numerical analysis of the landslide on RN12 at PK 119+000, ADEKAR, Béjaïa, Algeria, using MIDAS GTS NX software. Our rigorous methodology involved defining a representative geotechnical model, implementing a refined two-dimensional mesh, applying gravitational loads, and conducting a parametric study.

The novelty of this research rests in its dependence on a real-world case study, located along a roadway in the commune of ADEKAR, in the Béjaïa Province (Algeria) a region well known for its unstable slopes and frequent landslides. This region, characterized by rocky topography, clayey soils, and copious

rainfall, provides a good environment for assessing the efficiency of soil nailing under extreme natural circumstances. The findings obtained provide useful insights into the effect of each parameter on the safety factor.

2. Overview of the study area

2.1. The site's location and geology

The site investigated in this study is located in the municipality of Adekar (Béjaïa Province, Algeria) at PK 119+000 within the Djurdjura Mountain range. It is situated along National Road RN12, which connects the provinces of Béjaïa and Tizi Ouzou. The geographic location of the research site is illustrated via satellite imagery in Fig. 1. The site's coordinates are 36°43'31.91" N, 4°36'59.48" E, at an elevation of 3,177 ft.

The region under examination is situated in the southwestern sector of the Béjaïa Province, inside the structural realm of the Kabyle coastal chains, which contain the historic massifs of Grande and Petite Kabylie (Fig. 2). These geological units are largely made up of metamorphic rocks of Hercynian and Alpine origin, overlain by Cenozoic sedimentary deposits, and locally intruded by recent eruptive formations. This lithological composition represents a very complicated tectonic history, characterized by many orogenic phases and significant geodynamic activity [23].



Fig. 1. Satellite image (Google Earth) of geographical location of the landslide site

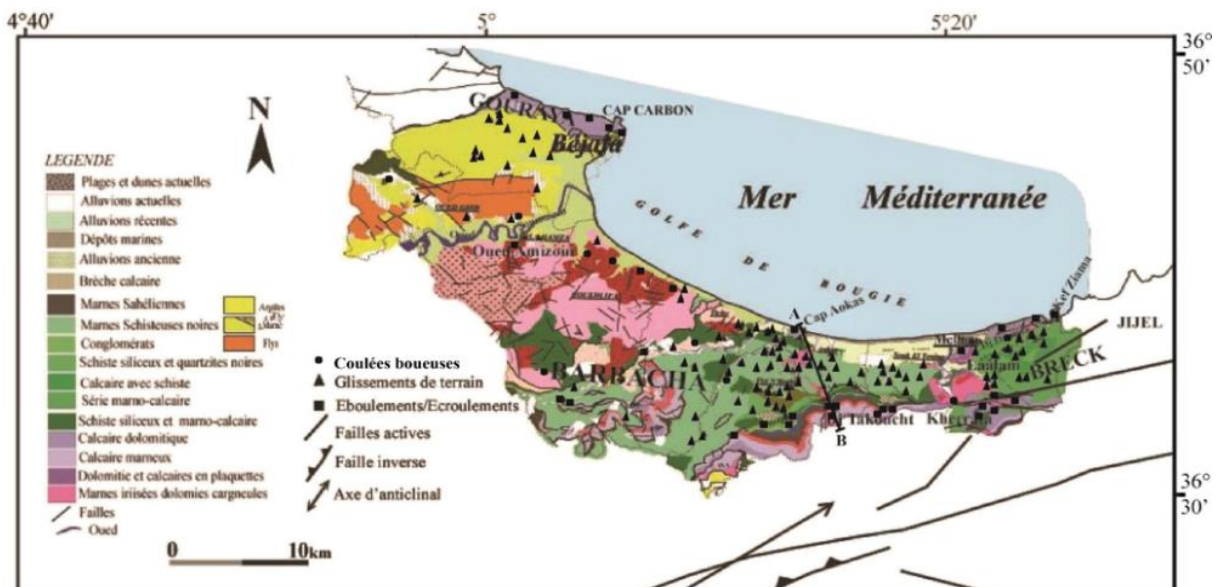


Fig. 2. Geological map of the city of Béjaïa (Algeria) [28]

The study area, which corresponds to a segment of National Road RN12, is primarily composed of Quaternary formations, notably ancient alluvial deposits and alluvial fan cones, distributed along the valley of the Oued Agrioun. These recent deposits, often the result of gravitational mass movements, are well documented within the seismotectonic zones of northern Algeria [24]. At certain locations, calcareous breccias and slope scree are also observed, derived from highly cemented Liassic and Jurassic debris. This type of rock is noted for its excellent construction quality due to its compactness and hardness. Such lithological facies have been extensively described in the karstic massifs of the Djurdjura range [25].

The Tertiary formations in the region are predominantly composed of Tellian nappes, which almost entirely blanket the southern coastal area of Béjaïa. Additionally, Numidian nappe outcrops—primarily made up of sandstones and flysch-like sequences—are also locally observed. The structural superposition of the Numidian and Tellian nappes has been documented in several tectono-stratigraphic studies focused on the Souk Ahras and Béjaïa regions [26]. In the segment under consideration, Cretaceous formations are also present, particularly those of the Neocomian Group, which consist of interbedded marly, calcareous, and siliceous series that are stratigraphically difficult to distinguish. Such sedimentary successions are characteristic of the internal margin of the Algerian Tellian Basin, as highlighted by Tissot [27]

2.2. Regional hydrogeology

Compared to other parts of the nation, this mountainous zone of Kabylia is distinguished by the diversity of its physical and natural settings. This variability originates from a highly dissected and rough terrain mixed with a rich hydrographic network, which together give rise to a mosaic of diverse landscapes and geosystems. The Djurdjuramassif crossed at PK 119+000 along the RN12 in the municipality of Adekar—represents a hydrogeologically crucial location due to the presence of both alluvial and karstic formations. The principal lithological units consist mostly of Quaternary alluvial terraces, marked by their high permeability and abundance of coarse materials such as sands and gravels. These unconsolidated deposits generate a weakly cohesive substratum that tends to

saturate fast during heavy rains, thus drastically lowering its mechanical cohesion and stability [29,30].

The significance of the hydrographic network amplifies surface runoff, leading to intense infiltration into unconfined aquifers. This process locally raises the water table, thereby reducing slope stability. Additionally, the overexploitation of groundwater resources in the Soummam Valley may cause abrupt fluctuations in piezometric levels, further exacerbating the risk of collapse in unconsolidated soils. These hydrogeological conditions make the region particularly vulnerable to landslide phenomena, especially during periods of intense rainfall, as demonstrated by several recent regional hydrogeological studies [31,32].

2.3. Description of the landslide at the study site

The investigated area extends over approximately 200 meters along the down slope section of the roadway (Fig. 3). The landslide is characterized by the development of a well-defined rupture surface along which mass displacements have occurred, indicating a large-scale failure in terms of mobilized volume. The slope instability is predominantly manifested at the lower part of the embankment, where a scarp approximately 1 meter high has formed at the road edge, accompanied by accumulation ridges (bulges) at the toe of the down slope embankment (Fig. 4). Additionally, tensile cracks of oblique orientation have developed along the pavement over a stretch of approximately 60 meters (Fig. 5), with variable aperture widths ranging from 1 to 2 cm. The affected road section exhibits a cut-and-fill profile, with a significant elevation difference between the road level and the toe of the slope, reaching up to 18 meters in height. The critical slope angle is estimated to be between 35° and 40°, with a maximum vertical displacement observed at 4.2 meters (Fig. 3). Visible distress and structural damage were recorded along the affected segment of the roadway, particularly at the toe of the embankment, indicating ongoing instability processes (Fig. 6). Notable observations include:

- Rupture of half of the roadway over a 50-meter stretch due to the landslide movement;
- Complete detachment and loss of the roadside shoulder;
- Collapse of the culvert and drainage structures on the lower part of the slope.

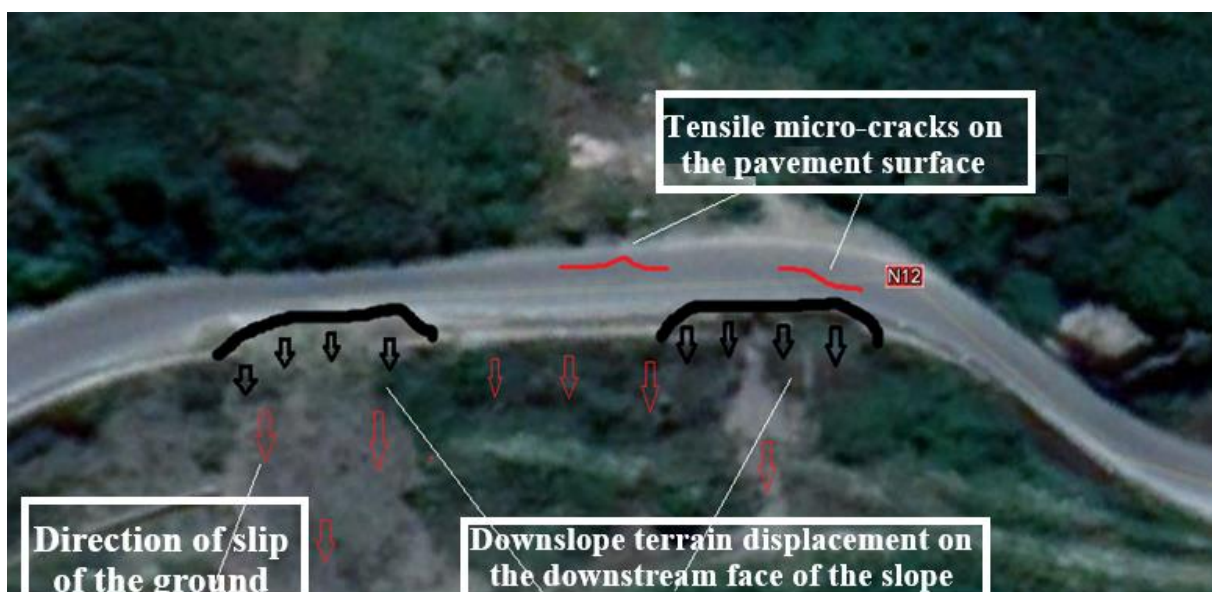


Fig. 3. The terrain under study morphological characteristics



Fig. 4. Shoulder collapse and embankment failure along the roadway



Fig. 5. Tensile microcracks along the pavement surface

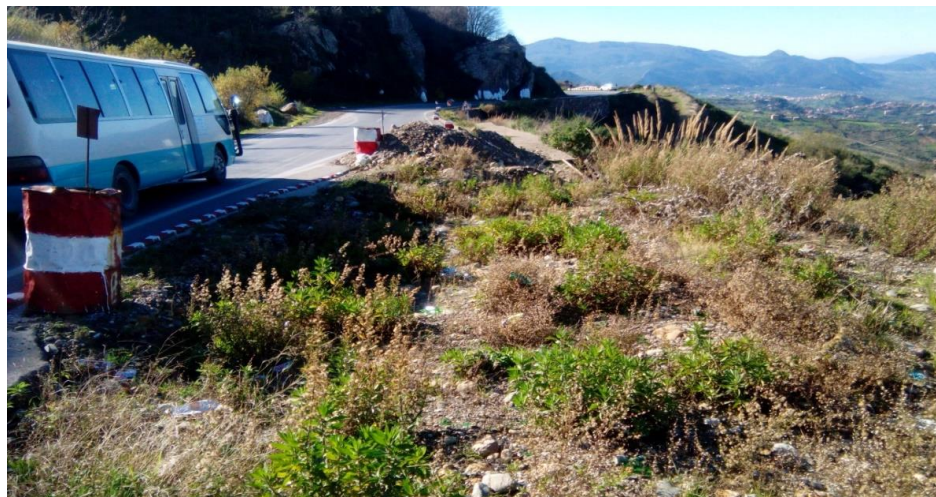


Fig. 6. Structural failures and pavement rupture along the half-carriageway section

3. Methodology

The methodology adopted in this study is structured into several phases. First, the slope geometry and the geotechnical properties of the soil were defined and implemented in the MIDAS GTS NX software using the Mohr–Coulomb constitutive model within a finite element analysis (FEA)

framework. This approach allowed a comprehensive assessment of slope stability, including the calculation of the Factor of Safety (FOS) and the identification of the potential failure surface (slip circle). Based on the obtained results, appropriate stabilization solutions were then selected and evaluated to ensure the

adequacy of the proposed design. To achieve the research objectives, the analysis was conducted in the following stages:

- Phase 1: Baseline Condition- Evaluation of the natural slope stability without external loads.
- Phase 2: Traffic Loading Impact- Assessment of slope behavior under the influence of road traffic loads.
- Phase 3: Reinforcement and Stabilization- Analysis of the slope’s stability after implementing soil nailing techniques.
- Phase 4: Parametric study- This phase is used to investigate the influence of mechanical properties on the factor of safety in slope stability analysis

3.1. Slope geometry and soil properties

The slope geometry and the corresponding finite element mesh generated using MIDAS GTS NX are presented in Fig. 7, while the associated geotechnical properties are summarized in Table 1. In the numerical simulations, the soil behavior was

represented using the Mohr–Coulomb constitutive model. The parameters listed in Table 1 were obtained from geotechnical investigations conducted by the Public Works Laboratory of Béjaïa, providing a reliable experimental basis for the numerical analysis.

3.2. Soil nail parameters

Table 2 presents the mechanical and geometrical characteristics of the soil nails used for slope reinforcement. The selected parameters such as nail length, diameter, spacing, inclination, and steel mechanical properties were determined based on the results of iterative numerical modeling. These parameters were chosen to ensure adequate load transfer between the soil and the reinforcement system, improve global slope stability, and satisfy the minimum safety requirements prescribed by national regulations, while also maintaining constructability and cost-effectiveness under the site-specific conditions.

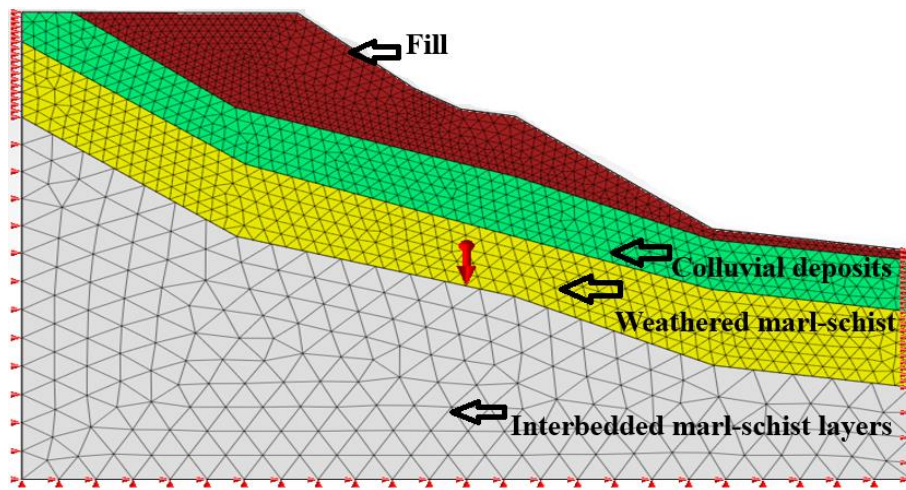


Fig. 7. Discretized slope geometry generated in Midas GTS NX

Table 1. Physical and mechanical properties of the soils at the study site

Layer No.	Soil Type	Constitutive Model	Young’s Modulus (kPa)	Unit weight (kN/m ³)	Poisson’s Ratio (-)	Cohesion (kPa)	Friction Angle (°)
1	Fill	Mohr- Coulomb	15000	17.5	0.30	15	30
2	Colluvial deposits	Mohr- Coulomb	47000	20.0	0.30	33	38
3	Weathered marl-schist	Mohr- Coulomb	42000	20.1	0.30	60	15
4	Interbedded marl-schist layers	Mohr- Coulomb	58000	21.2	0.30	500	20

Table 2. Mechanical and elastic properties of soil nail reinforcement

Material Type	Young’s Modulus (MPa)	Unit weight (kN/m ³)	Poisson’s Ratio (-)	Diameter (m)	Length (m)	Spacing (m)	Number of Nails
Elastic	210	78	0.20	0.025	10	2	7

4. Results and discussion

In this section, the phases outlined above were modeled using GTSNX software. To evaluate the effectiveness of soil nailing as slope reinforcement, the results of the first three phases were compared. This analysis focused on the resulting Factors of Safety (FOS) and the variations in slip circle geometry.

4.1. Phase 1 - Baseline condition without traffic loading

In the initial analysis phase, the slope was assessed under natural conditions without any applied traffic loading to establish a baseline stability condition. The numerical model, illustrated in Fig. 7, incorporates mesh discretization, boundary conditions, and self-weight loading to realistically represent the in-situ stress

state. The results, shown in Fig. 8, indicate that vertical displacements remain limited under gravity loading alone, with a calculated Factor of Safety (FOS) of 1.86. This value suggests a marginally stable slope in its natural state, implying that additional external loads or adverse environmental conditions could significantly reduce stability.

Figure 9 illustrates the distribution of plastic deformation zones within the slope under natural loading conditions, revealing localized plastic points mainly concentrated near the slope toe. These zones suggest the initiation of shear deformation along a potential slip path; however, no continuous failure surface is observed. The computed safety factor of approximately 1.85 confirms that the slope remains globally stable under self-weight conditions. The limited and non-progressive nature of the plastic deformations indicates that the slope exhibits adequate

resistance to gravitational forces in the absence of external surcharges. Overall, the results demonstrate that, although the slope is close to a critical state, its stability is maintained under natural conditions.

4.2. Phase 2 -Slope behavior under road traffic loading

In the second phase of the simulation, a uniform vehicular traffic surcharge of 37.14 kN/m² was applied to the roadway platform (Fig. 10). The results (Fig. 11) show that the traffic load significantly affects the slope's behavior, reducing the Factor of Safety from 1.82 under natural conditions to 1.303. This indicates a notable decrease in stability and highlights the critical impact of external loading on the slope.

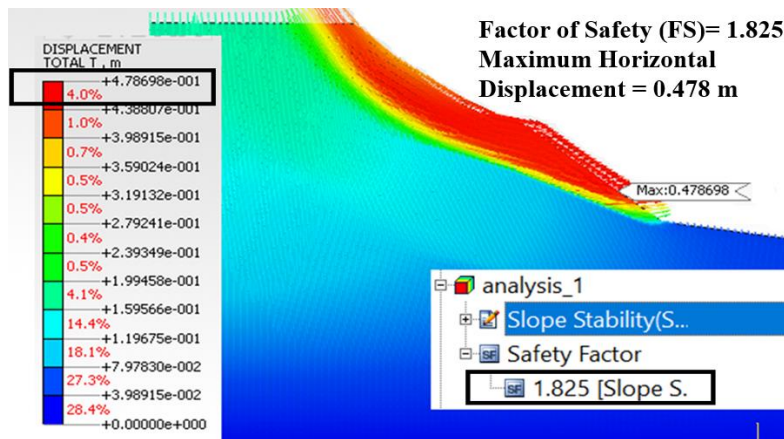


Fig. 8. Total displacement and factor of safety under natural slope conditions

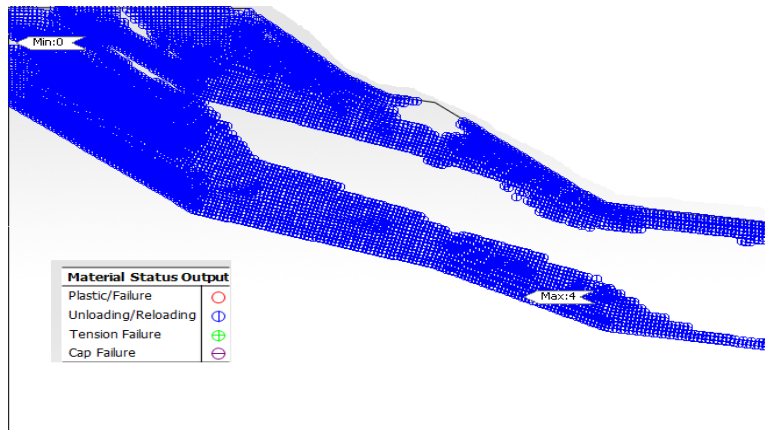


Fig. 9. Plastic point distribution and potential failure surface (Phase 1)

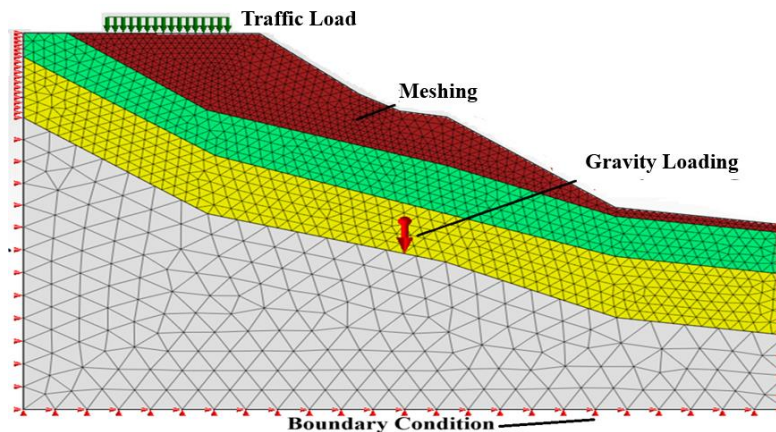


Fig. 10. Geometry, mesh, and applied loads of the Phase 2 model

Figures 12 and 13 illustrate the development of plastic deformation within the slope under traffic-induced loading. The emergence of a well-defined failure plane and the concentration of plastic points along preferential shear zones indicate a progressive reduction in shear strength and a decrease in slope

stability. These visualizations highlight potential instability zones and demonstrate how external loading redistributes stresses, supporting the observed reduction in the Factor of Safety in Phase 2.

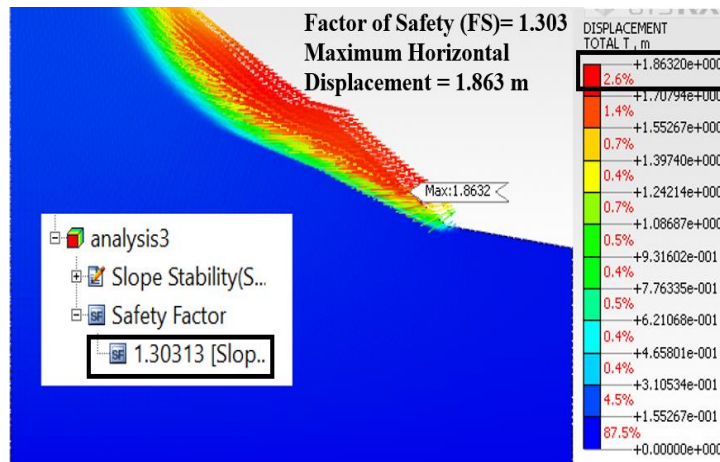


Fig. 11. Computed factor of safety for the slope under traffic surcharge (Phase 2)

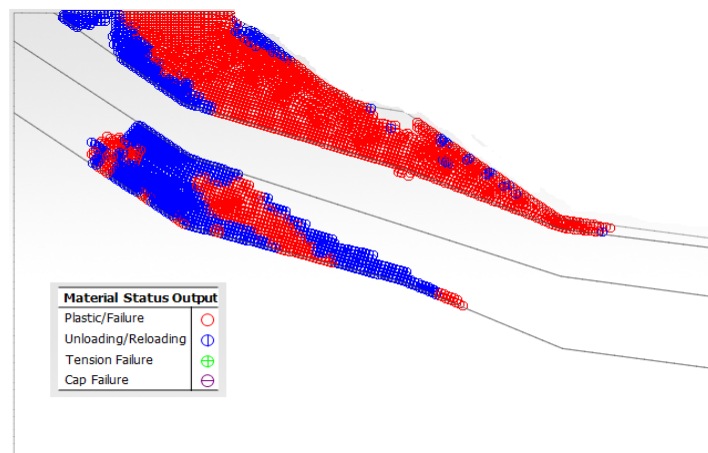


Fig. 12. Plastic point distribution and failure plane under traffic load

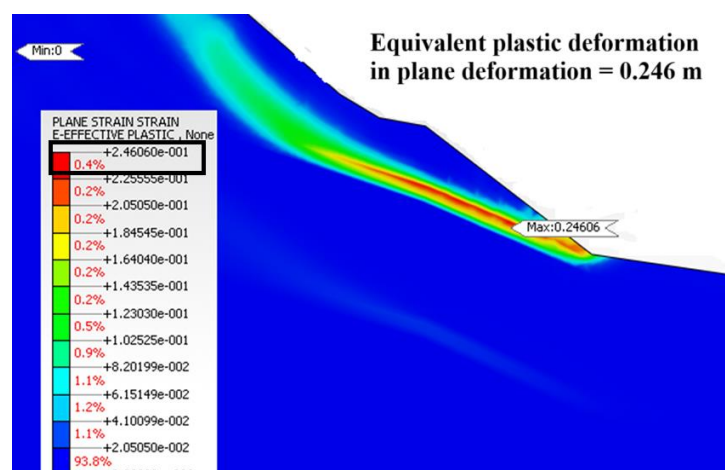


Fig. 13. Equivalent plastic strain under plane strain conditions

The comparison of the two simulation phases highlights the slope's high sensitivity to external loading. Under self-weight (Phase 1), the slope is relatively stable, with a maximum vertical displacement of 0.47 m and a Factor of Safety of 1.82. Introducing the vehicular surcharge (Phase 2) reduces the Factor of Safety to 1.303, indicating a critical approach to failure. These

results demonstrate the significant destabilizing effect of traffic loads, especially in layered or weathered soils, and emphasize the importance of considering live loads in slope stability assessments. Static analysis alone may underestimate real-world behavior, justifying the use of reinforced stabilization measures (Fig. 14)

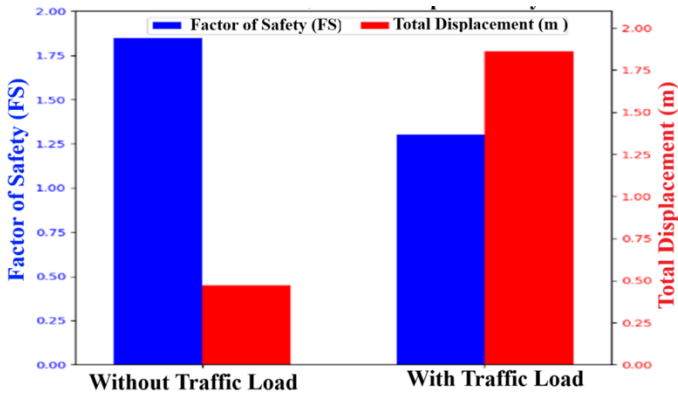


Fig. 14. Effect of traffic load on slope stability

Table 3. Summary of computed Factors of Safety

Condition	Factor of Safety (FS)
Without surcharge	1.82
With 37.14 kN/m ² surcharge	1.303

4.3. Phase 3: Soil nailing for slope stabilization

In this context, the initial solution proposed by a geotechnical consultancy involved the construction of a gabion

wall at the toe of the slope, an approach recognized for its structural robustness but also associated with high costs and a significant visual impact. This study proposes an alternative solution based on soil nailing reinforcement, as shown in Fig. 15, a more discreet and potentially cost-effective technique. Its effectiveness is assessed through a series of detailed numerical simulations designed to compare different configurations and determine the most efficient and contextually appropriate stabilization strategy. The required nail parameters are summarized in Table 2.

The soil nailing reinforcement significantly improved slope stability, increasing the safety factor from 1.303 to 1.901, well above the typical design threshold of $FS \geq 1.5$. The maximum axial force in the nails, approximately 144.9 kN, remains well below the steel's elastic limit of 245.5 kN, primarily concentrated in the lower portion of the rightmost nail. The force distribution indicates that the reinforcement progressively engages with the soil and adapts to internal deformations. The installation of seven 25 mm-diameter nails spaced at 2 m intervals effectively enhanced the slope's mechanical performance, demonstrating the structural adequacy and effectiveness of this stabilization strategy under external loading.

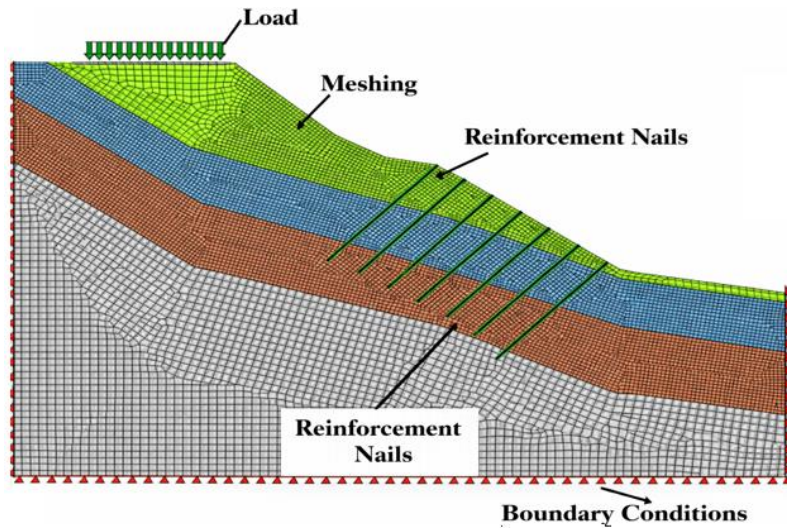


Fig. 15. Geometry, mesh, and loading conditions of the model

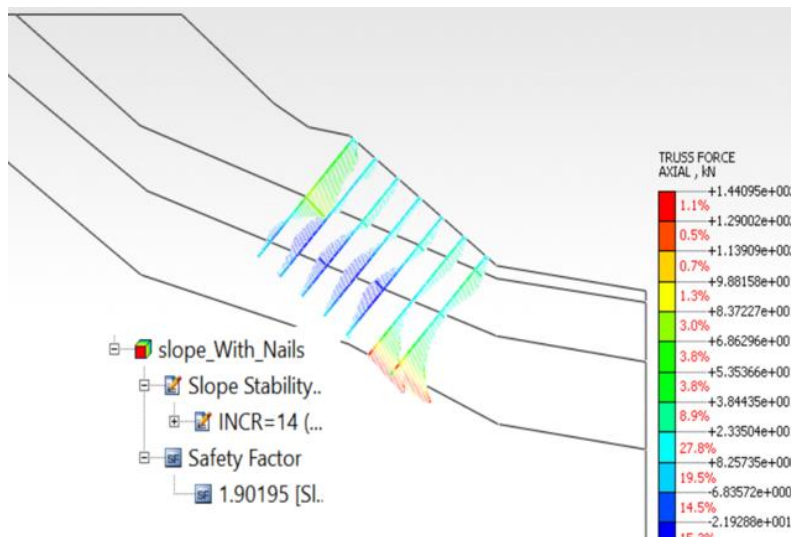


Fig. 16. Axial force distribution within the reinforcement nails

Table 4. Summary of the results illustrating the effect of Soil Nailing

Condition	Factor of Safety (FS)	Max Nail Force (kN)
Unreinforced & Traffic Load	1.303	–
Reinforced with Soil Nails	1.901	144.09

Table 5. Mechanical parameters used in the parametric study (Effect of cohesion)

Mechanical Parameters	Case 1	Case 2	Case 3	Case 4
Cohesion (kPa)	5	10	15	20
Friction Angle (°)	25	25	25	25

4.4. Parametric study

To enhance the effectiveness of slope stabilization strategies, it is essential to develop a rigorous understanding of the impact of geomechanical parameters on the overall stability of the system. Accordingly, an advanced parametric analysis was conducted to systematically evaluate the sensitivity of the Factor of Safety (FOS) to variations in critical soil properties. Two fundamental mechanical parameters were investigated: the internal friction angle (ϕ), which characterizes the soil's resistance to shear stress through intergranular friction, and cohesion (c), which represents the component of shear strength independent of normal stress, particularly significant in fine-grained soils with high clay content. These parameters are critical in understanding and predicting slope performance under operational loading conditions.

4.4.1. Effect of embankment cohesion under a traffic load

This study investigates the effect of embankment soil cohesion on slope stability under a uniform static surcharge of 37.14 kN/m². Numerical simulations were performed with a constant internal friction angle ($\phi = 25^\circ$) while varying cohesion (c) from 5 to 20 kPa. The selected cases are summarized in Table 5.

The results illustrated in Fig. 17 correspond to the scenario with low soil cohesion ($C = 5$ kPa) and an internal friction angle of 25° . The numerical simulation yields a Factor of Safety (FS) of 1.065, which approaches the critical threshold of instability.

The parametric analysis conducted on four slope configurations differing solely in the cohesion value ($c = 5, 10, 15,$ and 20 kPa) with a constant internal friction angle ($\phi = 25^\circ$) has provided valuable insights into the influence of soil cohesion on slope behavior under static surcharge loading (Fig. 10). Figure 21 illustrates the evolution of total displacement and the corresponding Factor of Safety (FS) across the analyzed cases. The results demonstrate a consistent enhancement in global stability as cohesion increases. For the lowest cohesion value ($c = 5$ kPa), the slope exhibited critical performance, with a maximum displacement exceeding 0.84 m and an FS of 1.293, indicating proximity to failure conditions. As cohesion increased to 10 and 15 kPa, displacement values were reduced to 0.76 m and 0.65 m respectively, while the FS improved to 1.365 and 1.388, reflecting gradual stabilization. The case with the highest cohesion ($c = 20$ kPa) achieved the best performance, with a relatively lower maximum displacement of 0.732 m and an FS of 1.465.

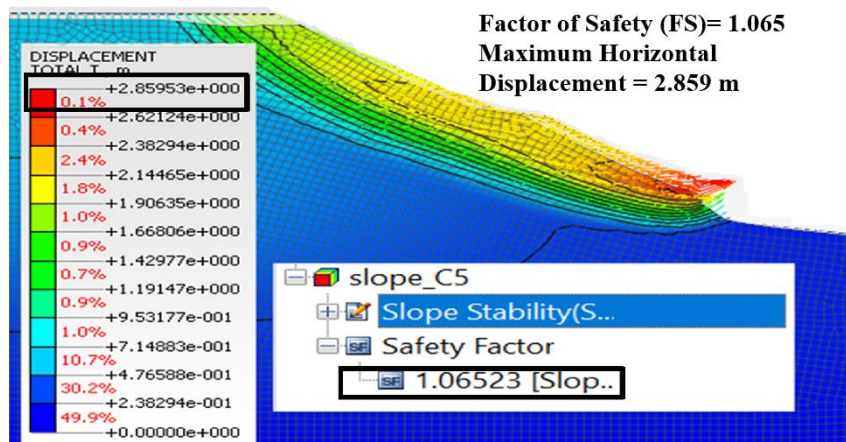


Fig. 17. Total displacement and computed safety factor for the case ($C = 5$ kPa, $\phi = 25^\circ$)

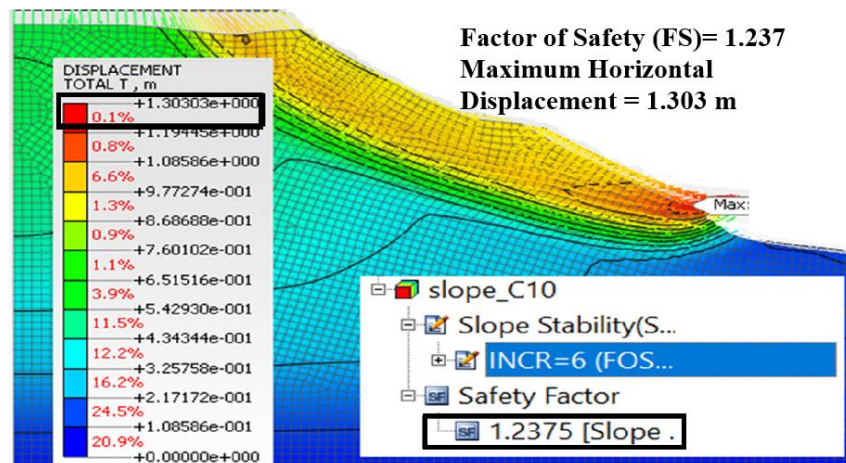


Fig. 18. Total displacement and safety factor values for the case ($C = 10$ kPa, $\phi = 25^\circ$)

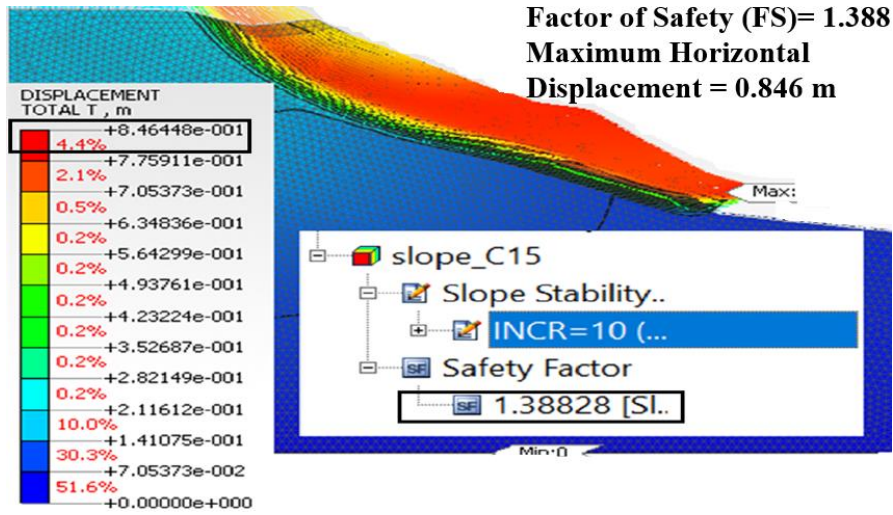


Fig. 19. Total displacement and safety factor values for the case ($C = 15 \text{ kPa}$, $\phi = 25^\circ$)

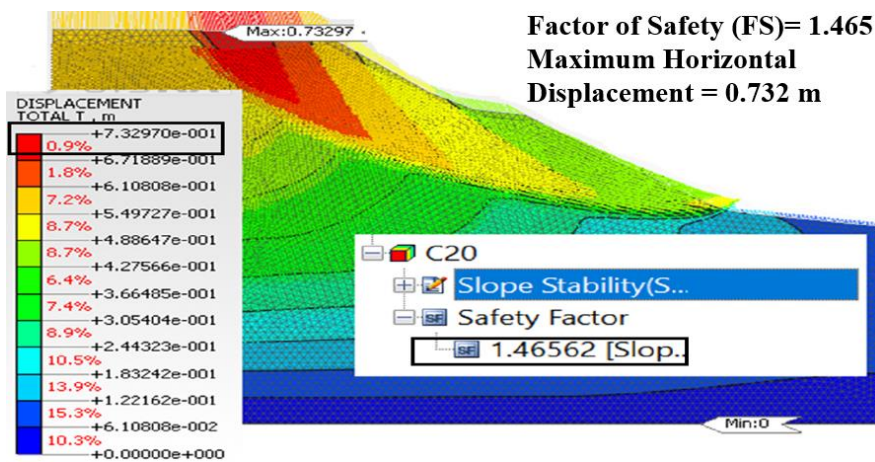


Fig. 20. Total displacement and safety factor values for the case ($C = 20 \text{ kPa}$, $\phi = 25^\circ$)

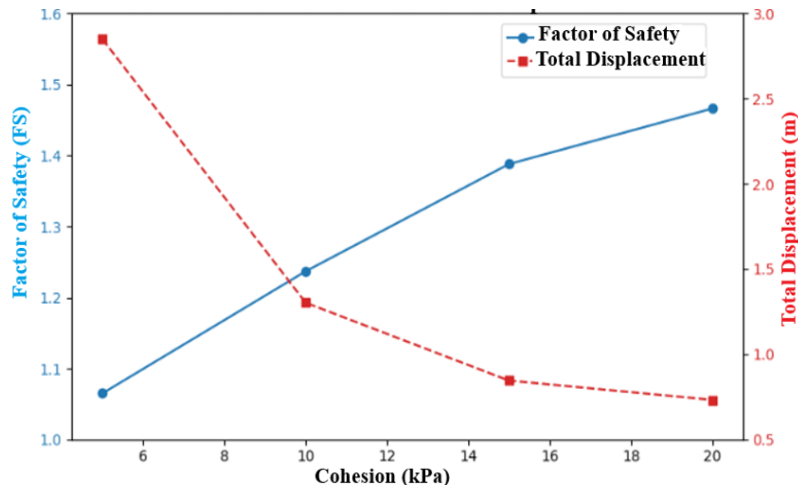


Fig. 21. Effect of cohesion on FS and total displacement

Table 6. Summary of the results illustrating the effect of cohesion ($\phi = 25^\circ$, Surcharge = 37.14 kN/m^2)

Case	Cohesion C (kPa)	Factor of Safety (FS)
1	5	1.065
2	10	1.237
3	15	1.388
4	20	1.465

4.4.2. Influence of friction angle (ϕ') on embankment stability

In this section, the study maintains a constant cohesion value of 5 kPa and applies a uniform linear surcharge of 37.14 kN/m^2 . Three simulation cases were analyzed with friction angles varying from 30° to 40° , enabling a rigorous assessment of how incremental increases in ϕ affect the mechanical performance of the embankment. The mechanical properties adopted in this analysis are presented in Table 7.

Table 7. Mechanical parameters used in the parametric study (Effect of ϕ)

Mechanical Parameters	Case 1	Case 2	Case 3
Cohesion (kPa)	5	5	5
Friction Angle ($^{\circ}$)	30	35	40

Figure 25 presents the influence of the internal friction angle (ϕ) on the Factor of Safety (FS) of embankments modeled with a constant cohesion of 5 kPa under linear surcharge loading. A clear positive correlation is observed between increasing ϕ and

the FS, while displacement shows a monotonic decrease. Specifically, as ϕ increases from 30° to 40° , the FS improves significantly from 1.203 to 1.650, while the corresponding total displacement declines from 0.2311 m to 0.145 m. This trend underscores the dominant role of frictional resistance in enhancing global slope stability and minimizing deformation, reaffirming the importance of precise geotechnical characterization for safe and efficient design.

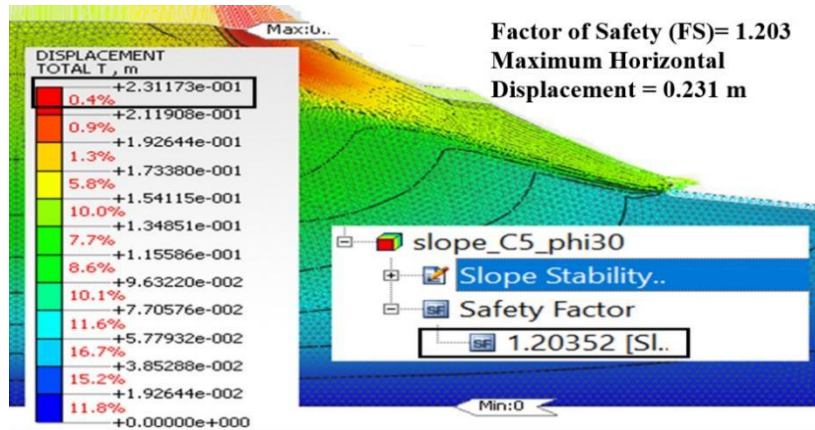


Fig. 22. Total displacement and safety factor values for the case ($C = 5$ kPa, $\phi = 30^{\circ}$)

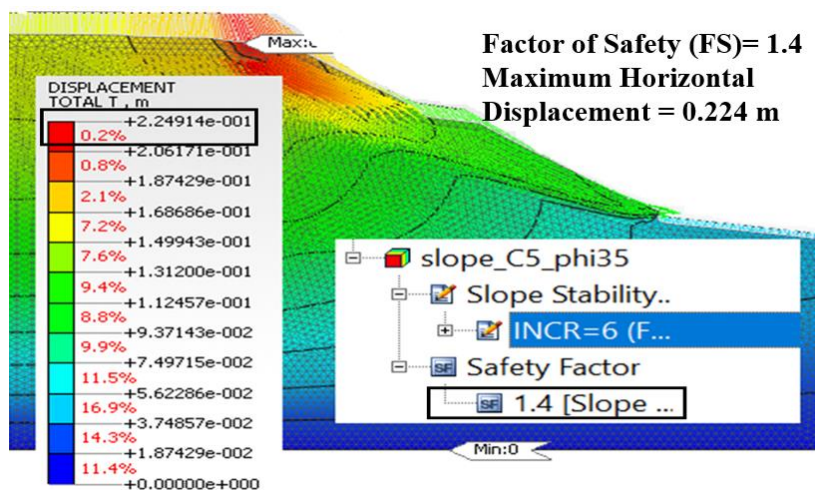


Fig. 23. Total displacement and safety factor values for the case ($C = 5$ kPa, $\phi = 35^{\circ}$)

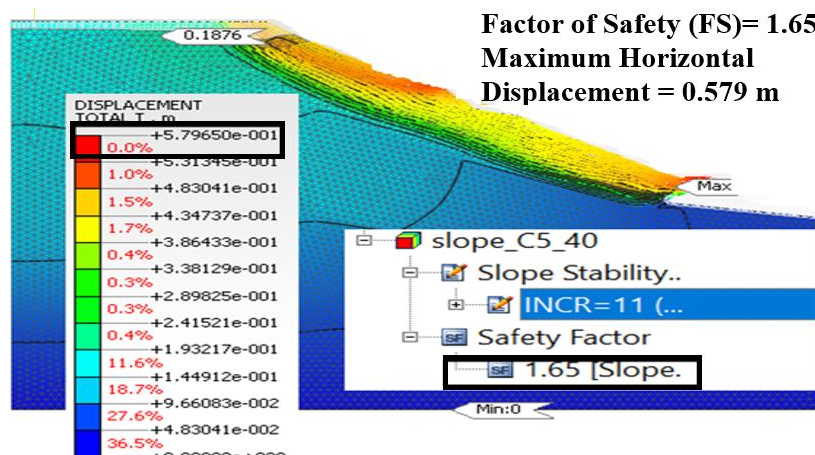


Fig. 24. Total displacement and safety factor values for the case ($C = 5$ kPa, $\phi = 40^{\circ}$)

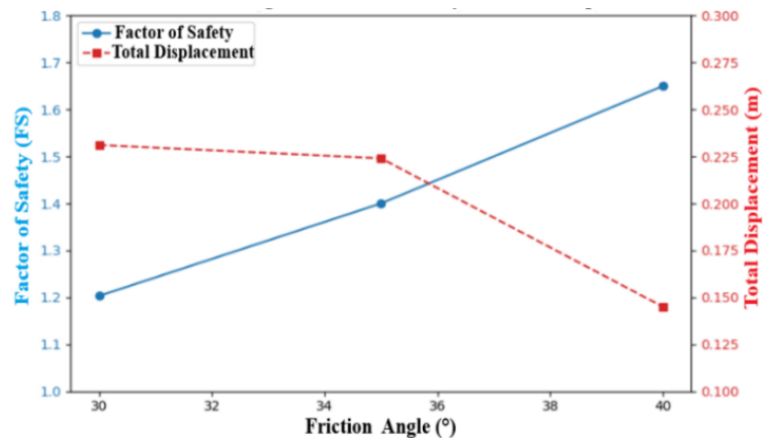


Fig. 25. Effect of friction angle on factor of safety and total displacement

Table 8. Summary of the results illustrating the influence of the friction angle

Case	Friction Angle ϕ (°)	Factor of Safety (FS)
1	30	1.203
2	35	1.400
3	40	1.650

5. Conclusions

The study conducted on the slope located in the municipality of Adekar, within the Béjaïa Province, rigorously and quantitatively demonstrated the significant contribution of soil nailing techniques in enhancing slope stability under constrained conditions (steep topography, road surcharge, heterogeneous soil composition). Through precise numerical modeling based on the finite element method using MIDAS GTS NX software, multiple reinforcement and loading configurations were simulated, enabling a detailed assessment of the mechanical responses of the slope.

The results clearly indicate that, in its initial state, the slope exhibited critical instability, with a Factor of Safety (FS) of 1.303 under vehicular loading and horizontal displacements reaching 1.86 m. However, after implementing seven soil nails of 10 m length, 25 mm diameter, and spaced 2 m apart, the FS increased to 1.901. This substantial improvement confirms the effectiveness of soil nailing as a reliable, durable, and economically viable stabilization solution, particularly in contexts where traditional methods, such as gabion walls, prove limited.

Moreover, the parametric analysis highlighted the critical influence of soil mechanical properties on global stability. Progressive increases in soil cohesion (from 5 to 20 kPa) and internal friction angle (from 30° to 40°) resulted in a marked enhancement of the FS (up to 1.65) and a corresponding reduction in deformations. These findings emphasize the importance of thorough geotechnical characterization during the design phase.

The analysis of axial force distribution within the reinforcement nails revealed differential stress patterns depending on their spatial positioning. This suggests the need for optimized, location-specific design approaches. A refined understanding of local stress behavior could support the integration of complementary techniques, such as geogrids, shotcrete, or micropiles, in highly stressed zones to further improve performance.

Finally, future research should incorporate dynamic load conditions (e.g., railway traffic, seismic activity) and experimental studies on physical models to validate numerical predictions and refine stabilization strategies, particularly by accounting for material heterogeneity and coupled hydro-mechanical effects.

This study confirms that the combined use of soil nailing and advanced numerical modeling provides an effective and optimized framework for the safe and sustainable design of retaining structures in geologically unstable environments.

References

- [1] Li H., Samsudin N.A., A systematic review of landslide research in urban planning worldwide. *Natural Hazards* 121 (2024) 6391–6411. <https://doi.org/10.1007/s11069-024-07064-4>
- [2] Fang Z., Wang Y., van Westen C., Lombardo L., Landslide hazard spatiotemporal prediction based on data-driven models: Estimating where, when and how large landslide may be. *International Journal of Applied Earth Observation and Geoinformation* 126 (2024) 103631. <https://doi.org/10.1016/j.jag.2023.103631>
- [3] Baziz F., Bahloul O., Baziz N., The impact of construction activities on the stability of highway slopes. *Engineering, Technology & Applied Science Research* 15(1) (2025) 19115–19120. <https://doi.org/10.48084/etasr.9185>
- [4] Qin H., Yin X., Tang H., Cheng X., Reliability analysis and geometric optimization method of cut slope in spatially variable soils with rotated anisotropy. *Engineering Failure Analysis* 158 (2024) 108019. <https://doi.org/10.1016/j.engfailanal.2024.108019>
- [5] Bourdim S.M.E.A., Chekroun L.E.H., Benanane A., Bourdim A., Treatment of a landslide by using piles system, case study of the East-West Highway of Algeria. In *International Congress and Exhibition Sustainable Civil Infrastructures: Innovative Infrastructure Geotechnology*, 2017, 16–24, Cham: Springer International Publishing. https://doi.org/10.1007/978-3-319-63543-9_2
- [6] Wang Z., Butt J.A., Huang S., Medic T., Wieser A., Dense 3D displacement estimation for landslide monitoring via fusion of

- TLS point clouds and embedded RGB images. *arXiv preprint* (2025) 2506.16265. <https://doi.org/10.48550/arXiv.2506.16265>
- [7] Albanwan H., Qin R., Liu J.K., Remote sensing-based 3d assessment of landslides: A review of the data, methods, and applications. *Remote Sensing* 16(3) (2024) 455. <https://doi.org/10.3390/rs16030455>
- [8] Hallal N., Hamidatou M., Hamai L., Aguemoune S., Lamali A., Landslides triggered by the August 2020 Mw 5.0 Mila, Algeria, earthquake: spatial distribution and susceptibility mapping. *Euro-Mediterranean Journal for Environmental Integration* 9(3) (2024) 1063-1085. <https://doi.org/10.1007/s41207-024-00471-w>
- [9] Zolqadr E., Yasrobi S.S., Olyaei M.N., Analysis of soil nail walls performance-case study. *Geomechanics and Geoengineering* 11(1) (2016) 1-12. <https://doi.org/10.1080/17486025.2015.1006263>
- [10] Kumar S., Roy L. B., Investigating the slope stability and factor of safety properties of soil reinforced with natural jute fibers under different rainfall conditions. *Engineering, Technology & Applied Science Research* 13(1) (2023) 9919-9925. <https://doi.org/10.48084/etasr.5481>
- [11] Indratmoko S., Koestoeer R.H., Landslide characteristics triggering evacuations: A comparative study of community responses and disaster management approaches. *Calamity: A Journal of Disaster Technology and Engineering* 2(2) (2025) 100-115. <https://doi.org/10.61511/calamity.v2i2.2025.1437>
- [12] Rahardjo H., Ong T.H., Rezaur R.B., Leong E.C., Factors controlling instability of homogeneous soil slopes under rainfall. *Journal of Geotechnical and Geoenvironmental Engineering* 133(12) (2007) 1532-1543. [https://doi.org/10.1061/\(ASCE\)1090-0241\(2007\)133:12\(1532\)](https://doi.org/10.1061/(ASCE)1090-0241(2007)133:12(1532))
- [13] Sharma M., Samanta M., Sarkar S., Soil nailing: an effective slope stabilization technique. In: *Landslides: Theory, Practice and Modelling* (2018) 173-199. https://doi.org/10.1007/978-3-319-77377-3_9
- [14] Bathini D.J., Krishna V.R., Performance of soil nailing for slope stabilization-a review. *IOP Conference Series: Earth and Environmental Science* 982 (2022) 012047. <https://doi.org/10.1088/1755-1315/982/1/012047>
- [15] Marwane H., Mohamed E.H., Mohammed M., Bensaid M., Kamal B., Mohammed A., Morabit A., Soil nailing for slope stabilization: an overview. *Interactions* 246(1) (2025) 1-23. <https://doi.org/10.1007/s10751-024-02234-z>
- [16] Srivastava S., Sharma A.K., Nayak S., A comparative analysis of slope stability based on advanced machine learning methods. In *Real-World Applications of AI Innovation* (2025) 277-306. <https://doi.org/10.4018/979-8-3693-4252-7.ch014>
- [17] Abdalhusein M.M., Al-Badran Y.M., Abd Hacheem Z., Almahmodi R.H., Mahmood M.S., AlMihna S.M.N., The effect of soil nailing inclination for improvement of gypsum sand soil in different slopes. *Operational Research in Engineering Sciences: Theory and Applications* 7(3) (2024). <https://oresta.org/menu-script/index.php/oresta/article/view/796>
- [18] Benayoun F., Boumezerane D., Bekkouche S.R., Ismail F., Optimization of geometric parameters of soil nailing using response surface methodology. *Arabian Journal of Geosciences* 14(19) (2021) 1965. <https://doi.org/10.1007/s12517-021-08280-z>
- [19] Imani Kalehsar R., Khodaei M., Dehghan A.N., Najafi N., Numerical modeling of effect of surcharge load on the stability of nailed soil slopes. *Modeling Earth Systems and Environment* 8(1) (2022) 499-510. <https://doi.org/10.1007/s40808-021-01087-7>
- [20] Zhang J., Luo C., Wu C., Lu M., Wu D., System reliability analysis of soil-nailed slopes. *Engineering Failure Analysis* 176 (2025) 109613. <https://doi.org/10.1016/j.engfailanal.2025.109613>
- [21] Elahi T.E., Islam M.A., Islam M.S., Parametric assessment of soil nailing on the stability of slopes using numerical approach. *Geotechnics* 2(3) (2022) 615-634. <https://doi.org/10.3390/geotechnics2030030>
- [22] Jaiswal S., Chauhan V. B., Influence of secondary reinforcement layers to enhance the stability of steep soil slope under earthquake loading. *Arabian Journal of Geosciences* 15(11) (2022) 1095. <https://doi.org/10.1007/s12517-022-10366-1>
- [23] Leprêtre R., de Lamotte D.F., Regional synthesis and progress on the geological research in north Africa. In: *The Geology of North Africa (2024) 1-19*. https://doi.org/10.1007/978-3-031-48299-1_1
- [24] Benhamouche A., Nedjari A., Bouhadad Y., Machane D., Oubaiche E., Sidi Said N., Field evidence of seismites in Quaternary deposits of the Jijel (Eastern Algeria) coastal region. *Journal of Seismology* 18(2) (2014) 289-299. <https://doi.org/10.1007/s10950-013-9384-1>
- [25] Quinif Y., Contribution à l'étude des cavités karstiques du Djurdjura (Algérie). Description morpho-hydrogéologique et cadre évolutif. *International Journal of Speleology* 10(2) (1978) 1. <http://dx.doi.org/10.5038/1827-806X.10.2.1>
- [26] Chabbi A., Chouabbi A., Chermiti A., Youssef M.B., Kouadria T., Ghanmi M., La mise en évidence d'une nappe de charriage en structure imbriquée : cas de la nappe tellienne d'ouled driss, Soukahras, Algérie. *Courrier du savoir* 21 (2016) 149-156.
- [27] Arab M., Rabineau M., Déverchère J., Bracene R., Belhai D., Roure F., Marok A., Bouyahiaoui B., Granjeon D., Andriessen P., Sage F., Tectonostratigraphic evolution of the eastern Algerian margin and basin from seismic data and onshore-offshore correlation. *Marine and Petroleum Geology* 77 (2016) 1355-1375. <https://doi.org/10.1016/j.marpetgeo.2016.08.021>
- [28] Kessasra F., Benabes D., Seraoui S., Chetibi N.E.H., Mesbah M., Khaled-Khodja S., Foughalia A., Groundwater flow and chloride transport modeling of the alluvial aquifer of lower Soummam Valley, Béjaia, North-East of Algeria. *Journal of African Earth Sciences* 173 (2021) 104023. <https://doi.org/10.1016/j.jafrearsci.2020.104023>
- [29] Kessasra F., Mesbah M., Khemissa Z., Bouab N., Khaled-Khodja S., Lamari H., Combined hydrogeological and nitrate modelling to manage water resources of the Middle Soummam Aquifer, Northeast of Algeria. *Arabian Journal of Geosciences* 10(16) (2017) 368. <https://doi.org/10.1007/s12517-017-3160-4>
- [30] Ghodbane M., Benaabidate L., Boudoukha A., Gaagai A., Adjissi O., Chaib W., Aouissi H.A., Analysis of groundwater quality in the lower Soummam Valley, North-East of Algeria. *Journal of Water and Land Development* 54 (2022) 1-12. <https://doi.org/10.24425/jwld.2022.141549>
- [31] Benabbes D., Kessasra F., Foughalia A., Kerouaz M., Abdellouch E.A., Khemissa Z., Coupled hydrogeological modeling and nitrate transport modeling to assess vulnerability pollution in an anthropized watershed, case study of the lower Soummam valley (Bejaia Northeast of Algeria). *Research Square* (2022). <https://doi.org/10.21203/rs.3.rs-1936780/v1>
- [32] Iftikhar A.A., Artati H.K., Finite element modelling of soil nailing inclination effect on slope stability: Cibereum slope case study. *Teknisia* 29(1) (2024) 14-23. <https://doi.org/10.20885/teknisia.vol29.iss1.art2>